

GREEN SYNTHESIS OF *MATRICARIA CHAMOMILLA* - DERIVED METAL NANOPARTICLES AND THEIR APPLICATIONS

Delia Maria Luca^a, Lăcrămioara Oprică^{a*},
Marius-Nicușor Grigore^b

^a*Faculty of Biology, “Alexandru Ioan Cuza” University,
20A Carol I Bd, Iasi 700506, Romania*

^b*Doctoral School of Biology, “Alexandru Ioan Cuza” University,
20A Carol I Bd, Iasi 700506, Iasi, Romania*

Abstract: This review explores the green synthesis of metal nanoparticles derived from *Matricaria chamomilla*, commonly known as chamomile, and investigates their potential applications. Utilizing an eco-friendly approach, chamomile extracts serve as both reducing and stabilizing agents in the synthesis process, resulting in the formation of nanoparticles (NPs) with unique properties with remarkable physicochemical and biological properties. Characterization techniques, including UV-Vis spectroscopy, transmission electron microscopy (TEM), Scanning Electron Microscopy (SEM) and X-ray diffraction (XRD), and Fourier Transform Infrared Spectroscopy (FTIR) confirm the successful synthesis and reveal information about morphology of the nanoparticles (size and shape), zeta potential, and formed bonds. The synthesized metal nanoparticles exhibit significant antibacterial, antifungal, cytotoxic, antioxidant, and catalytic activities, highlighting their potential as effective agents in biomedical and environmental applications.

Keywords: chamomile, green synthesis, metal nanoparticles, biological properties

*Lăcrămioara Oprică, *e-mail:* lacramioara.oprica@uaic.ro

Introduction

The field of green nano-technology is in continuous development, driven by the multifunctional properties of synthesized nanoparticles (NPs) across various industries.¹⁻⁵ Green synthesis presents a sustainable alternative to traditional chemical and physical methods, reducing the reliance on toxic chemical compounds, minimizing environmental pollution and associated harm.^{6,7} Additionally, green synthesis has been found to be cost-effective due to the use of biological resources such as plant or microbial extracts, eliminating the need for costly and “time-consuming” purification steps associated with chemical synthesis.⁸ Furthermore, biological extracts serve as natural reducing and capping agents, enhancing NPs stability and biocompatibility, making them suitable for applications in biomedicine, agriculture, catalysis, environmental remediation and electronics.⁹

Matricaria chamomilla, commonly known as chamomile, is an annual plant belonging to the *Asteraceae* family and originally from Europa and Asia and is known for its diverse biological effects.¹⁰ According to recent findings, chamomile displays a wide range of biological activities including antimicrobial, antioxidant, antiparasitic, insecticidal, antidiabetic, anti-allergic, anti-anxiety, anti-depressant, gastroprotective, anticancer, and anti-inflammatory effects.¹¹

Moreover, more than 120 phytoconstituents have been identified in chamomile, including terpenoids, phenolic compounds (e.g., flavonoids, phenolic acids), coumarins, alkaloids and several other phytochemicals that contribute to its biological value. It is known that flavonoids and phenolics, among other antioxidants, are primarily responsible for the reduction of metal ions and the stabilization of NPs during green synthesis.^{11,12} Due to the high concentration of these flavonoids and phenolic compounds in

chamomile extract, reaching up to 36.75 g quercetin equivalent /100 g, and 50.75 g gallic acid equivalent/100 g, respectively, chamomile has a promising candidate for use as a natural and capping agent in NPs synthesis.¹³ Additionally, chamomile is widely available, easily obtainable, and safe to handle.¹⁴ This review aims to evaluate the current state of NPs synthesis using different chamomile extracts, focusing on the synthesis methods employed, the main characteristics of the synthesized NPs (size, shape, and zeta potential) and their resulting properties and applications.

Chamomile-derived NPs biosynthesis method

The green synthesis of NPs using *M. chamomilla* generally involves four typical steps: preparation of the plant extract, preparation of the metal ion solution, mixing extract with metal ion solution and purification of the NPs. For instance (Figure 1, Table 1), AgNPs are the most commonly synthesized NPs, followed by other metal and metal oxide NPs, such as SiO₂ NPs, Magnetic NPs, Pd/Fe₃O₄ NPs, MgO NPs and MgO₂ NPs, CuO NPs, ZnO NPs, and TiO₂ NPs.^{9,15-20}

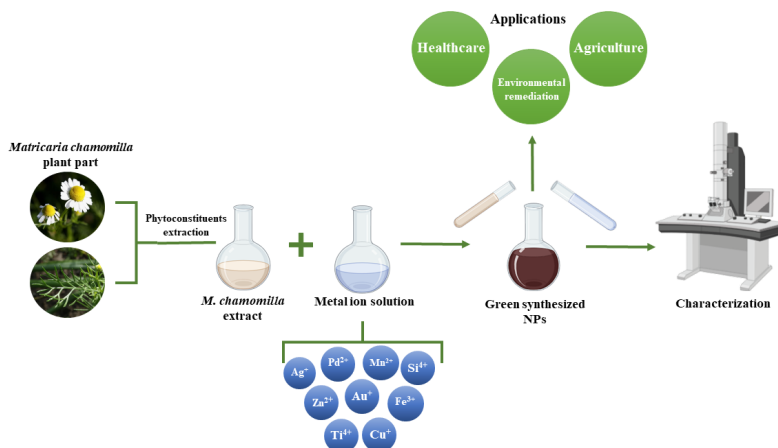


Figure 1. Summary of the synthesis, characterization and applications of metals derived from *Matricaria chamomilla* extracts.

According to the collected data (Table 1) flowers were the most frequently used plant part, followed by leaves, and aerial parts, which were utilized either in fresh or in powder form.^{12,14,15,18,19,21-24} Chamomile extracts were commonly prepared by boiling in various solvents (such as, distilled water, deionized water, ethanol, acetone or hydroalcoholic solution) or by sonication.^{12,15,20-22,25}

Subsequently, the metal ion solution was prepared, frequently using silver nitrate (AgNO_3) at a specific concentration (e.g., 1 mM to 20 mM).^{21,26} Other metal salt solutions used included sodium metasilicate (Na_2SiO_3), iron (III) chloride (FeCl_3), sodium tetrachloropalladate (Na_2PdCl_4), manganese acetate ($(\text{CH}_3\text{COOH})_2\text{Mn}$) and titanium tetraisopropoxide ($\text{Ti}(\text{C}_3\text{H}_7\text{O})_4$).^{9,15,16,20,27} In addition, some authors have used *Matricaria* sp. flower extract and ZnO to synthesize ZnONPs.¹⁹

The two solutions were then combined under controlled conditions, either at ambient temperature or under mild heating, with stirring or without agitation.^{12,26} Exposure to sunlight or storage in dark may further influence the NPs synthesis.^{17,23} The formation of NPs was indicated by a visible color change of the mixture, transitioning from colorless/yellowish shade into wine-red, yellow-brown, dark-brown or black color.^{12,21,22,25,28}

According to Alshehri and Malik, among the photosensitive phytoconstituents, the flavonoids (apigenin and apigenin-7-O-glucoside), and coumarins (luteolin and quercetin), act as reducing agents due to their hydroxyl (- OH) groups which facilitate the reduction of Ag^+ to Ag^0 .²³ Also, they mentioned that proteins from *M. chamomilla* play a role in capping and stabilization of NPs. The common method used for purification was centrifugation, followed by redispersion in a solvent. If necessary, multiple separation steps were performed to eliminate impurities.^{23,25}

Characterization of chamomile-derived NPs

For monitoring the formation and studying the characteristics of the chamomile-mediated NPs, various analytical techniques were used. UV-Visible spectroscopy (UV-Vis) reveals information about surface plasmon resonance peak, size and shape of NPs.

Scanning Electron Microscopy (SEM) and Transmission Electron Microscopy (TEM), X-ray Diffraction (XRD) are utilized to examine morphology, surface and internal structure and crystallinity. Fourier Transform Infrared Spectroscopy (FTIR) identifies functional groups and molecules associated with NPs. Dynamic Light Scattering (DLS) assesses particle size distribution in suspension and Zeta Potential Analysis evaluates surface charge and stability of NPs in colloidal systems.^{29,30}

Size and shape

AgNPs synthesized using chamomile extracts exhibit the most diverse size distribution, although all metal NPs predominantly display spherical morphology. For instance, Abdellatif et al. reported AgNPs with sizes up to approximately 115 ± 3.1 nm, while Alshehri and Malik achieved particles as small as 5 nm.^{12,23} Other chamomile-based NPs include SiO₂NPs ranging between 17 - 28 nm (TEM), Magnetite NPs of 6-8 nm (PXRD), ZnONPs between 8.9 - 32.6 nm (TEM), Pd/Fe₃O₄NPs of 20-50 nm (TEM), MgONPs and MgO₂NPs measuring 36.6-112.0 nm for (SEM) and CuONPs reaching sizes up to 140 nm (SEM).^{9,15-19}

It has been investigated how synthesis parameters, such as metal solution concentration, extract dosage and sunlight exposure influence AgNPs characteristics.²³ The findings indicated that higher metal ion

solution concentrations (2 mM) led to larger particles with a broader size distribution, while broader size distributions, 0.5 mM, promoted smaller and more uniform AgNPs.²³ Furthermore, a higher concentration of chamomile extract enhanced the availability of bioactive molecules responsible for reduction and stabilization, affecting both the size and shape. Similarly, Dogru *et al.* observed that higher volume of plant extract led to smaller AgNPs.²⁴ The pH also influences the size of biosynthesized NPs. Thus, Pakseresh *et al.* demonstrated that the size of TiO₂NPs increased in diameter, from 9 nm to 25 nm, when the medium became more alkaline.²⁰ Moreover, sunlight irradiation was found to accelerate the reduction process by activating photosensitive phytoconstituents, facilitating the formation of smaller particles. In contrast, reactions kept in the dark led to slower reduction rates, producing larger and less uniform particles.²³ In addition to chemical factors, physical parameters such as temperature and reaction time significantly influence the nucleation and crystal growth dynamics. For example, magnetite NPs synthesized with chamomile extract at 200 °C for 20 min yielded larger particles (S1) than at 260 °C for 5 min, which produced smaller NPs (S2).⁹ Studies have shown that smaller NPs exhibit enhanced biological effectiveness, such as antimicrobial and anticancer activity.^{9,24,31}

Zeta potential

Zeta (ζ) potential is a measure of colloidal stability, by measuring the electrostatic repulsion between particles.³² NPs synthesized using *M. chamomilla* extracts exhibited negative ζ values ranging from -18.5 mV to - 34 mV, suggesting good colloidal stability. The electrostatic repulsion that prevents aggregation and maintains dispersion stability.¹² Chamomile-

mediated NPs registered the following ζ potential: - 18.5 mV for ZnO NPs, - 20 mV for CuO NPs, - 31 mV for SiO₂ NPs and up to - 34 mV for Ag NPs.^{15,18,25,33}

Studies have noted that the phytochemical composition of plant extracts, metal salt solution concentration, and other parameters, such as pH and temperature can alter the surface charge and, thus, ζ potential. For instance, alkaline conditions and higher temperatures tend to decrease ζ values, whereas lower pH and lower temperatures tend to increase the ζ values, potentially leading to particle aggregation and colloidal instability.^{34,35}

Properties and Applications of *M. chamomilla*-based NPs

Antimicrobial properties

Pathogenic microorganisms pose a global challenge across various sectors, including health care and agriculture. Consequently, researchers are continuously exploring and optimizing potential treatments to mitigate the harmful effects of these microbes. Numerous studies have investigated the antimicrobial potential of chamomile-mediated NPs against both human pathogenic strains, such as *Staphylococcus aureus*, *Escherichia coli*, *Streptococcus mutans*, *Acinetobacter* sp., *Candida albicans* and phytopathogenic strains, including *Acidovorax oryzae*, *Ralstonia solanacearum*, and *Xanthomonas oryzae*.

Medical applications

Negahdary et al. observed that chamomile-mediated Ag NPs reduced the optical density of *S. aureus* in broth culture, and a similar inhibitory effect was observed on biofilm formation by *C. albicans*,

indicating antimicrobial activity.²⁶ Likewise, it has been reported a minimum inhibitory concentration (MIC) of 50 µg/ml chamomile-based Ag NPs against *Acinobacter* sp. Charm01, a common pathogen responsible for nosocomial infections.^{14,36} Furthermore, Dogru et al. demonstrated that smaller Ag NPs showed greater antimicrobial efficacy. Specifically, Ag NPs with diameters of 37 ± 4 nm, administered at a concentration of 50 ppm, reduced the cell density of *S. aureus* by ~90 %, *E. coli* by ~ 83 % and *C. albicans* by ~85 %. In contrast, larger particles (70 ± 5 nm and 52 ± 5 nm) achieved only ~ 72 % reduction.²⁴ Additionally, Ag NPs recorded an MIC of 56 ± 4.1 µg/mL and an inhibition zone (IZ) of 10.0 ± 1.0 mm against *S. mutans*, though less effective than ampicillin.²¹ Chamomile-based ZnONPs also displayed antibacterial activity against *S. aureus* and *E. coli*, with IZ values of 14 mm and 10 mm, respectively, following administration of 100 µg/mL.³³ Furthermore, MnO₂ NPs synthesized from chamomile and other plants extract showed promising antimicrobial activity against Gram-positive and Gram-negative bacteria, as well as fungal species. According to the findings, chamomile-based MnO₂ NPs exhibited moderate antimicrobial activity compared to the other synthesized NPs, inhibiting biofilm across all tested strains.²⁷

Agriculture safety

To evaluate the antibacterial potential of chamomile-mediated MgO NPs and MnO₂ NPs against *Acidovorax oryzae* strain RS-2, Ogunyemi et al. conducted MIC assay using 96-well microtiter plates with NPs concentrations of 4.0, 8.0 and 16 mg/mL.¹⁷ The highest concentration significantly reduced bacterial density by 62.90 % for MgO NPs and 71.25 % for MnO₂ NPs. TEM revealed that NPs disrupted the bacterial cell

membrane causing cytoplasmic efflux. Furthermore, the NPs suppressed the virulence by inhibiting biofilm formation and reducing swimming motility. In a separate study, Ogunyemi tested ZnO NPs synthesized using chamomile, olive leaves and red tomato fruit extracts against *Xanthomonas oryzae* pv. *oryzae*.³⁷ Maximum inhibition was observed at 16 µg/ml for all three samples, with antibacterial efficacy dependent on both particle size and administered concentration. Among these, the olive leaves-based ZnO NPs, which had the smallest particle size (48.2 nm), exhibited the highest antibacterial activity. Chamomile-mediated ZnO NPs also demonstrated significant antibacterial effects, including a 79.4 % suppression of biofilm formation and 62.4 % reduction of inhibition zone at 16 µg/ml. Similar alterations in bacteria cells were observed under TEM, as seen in the previous study. Another phytopathogenic bacterium, *Ralstonia solanacearum*, was found to be sensitive to ZnO NPs synthesized using chamomile extract.³⁷ According to Khan et al., ZnO NPs at the highest tested concentration (18 µg/ml) produced an IZ measuring 22.3 mm. Also, SEM study confirmed the damage to bacterial cells, including cell membrane deterioration, leakage of cytoplasm and cell deformation. Moreover, the presence of ZnO NPs in the soil not only mitigated disease severity but also enhanced plant growth.¹⁹ Additionally, it has been found that chamomile-derived SiO₂ NPs, when combined with chamomile extract, exhibited stronger inhibitory effects against *Aspergillus niger* (34 %) than chamomile extract alone (16 %). Interestingly, the chamomile extract alone exhibited a greater antifungal efficacy than the synthesized NPs against *A. niger* when tested independently.¹⁵ The authors suggest that the richness of phytochemicals in the extract may contribute to the alteration of fungal cell wall, interference with metabolic pathways, induction of stress response

and ultimately, fungal cell death.¹⁵ In addition, Shabir described that the NPs, such as ZnO NPs can penetrate the cell membrane by adhering to the plasmalemma, deteriorate microbial DNA due to ROS synthesis from Zn²⁺ ions, disrupt ATP production and DNA replication and reduce the virulence by interfering with carbon catabolic pathways.³³ Similarly, CuNPs synthesized from chamomile extract can interact with DNA molecules, acting as nucleases.¹⁸

Cytotoxic properties

Chamomile-based NPs have demonstrated significant cytotoxic effects against various cancer cell lines, including lung carcinoma cell lines (HLC-1, LC-2/ad, PC-14, A549), cervical cancer (HeLa), colon cancer (HCT116), colorectal cancer cells (SW620 and HT-29 cell lines), while exhibiting minimal toxicity toward healthy human cell lines such as embryonic (HEK293), skin (HaCaT) and fibroblast (HDF).^{12,22,25}

Ag NPs obtained using chamomile extract displayed great cytotoxic activity against A549 cells (lung cancer cells), with IC₅₀ values of 62.82 µg/mL and 42.44 µg/mL for 24 and 48 h, respectively. Treated cancer cells showed morphological alterations such as nuclear reduction, cellular fragmentation, chromatin condensation, nuclear shrinkage, formation of nuclear apoptotic structures and S phase cell cycle arrest.²⁵ Similarly, Yu et al. (2024) reported anticancer activity of chamomile-mediated AgNPs against three lung tumor cell lines, recording IC₅₀ values of 45µg/mL against HLC-1, 15 µg/mL for LC-2/ad and 14 µg/mL for PC-14 cells.²² In another study, chamomile-based AgNPs reduced the viability of colorectal cancer cells (SW620 and HT-29) at 20 µM concentration.¹² Paut et al. obtained two types of magnetic NPs (S1 and S2) under different

temperature and reaction time conditions, and due to their structural differences, S1 exhibited relatively uniform cytotoxicity against both healthy and cancer cells, while S2 displayed selective cytotoxicity with IC_{50} values ranging from 0.45 to 0.75 mg/mL for healthy cells and approximately 0.19 mg/mL for cancer cell lines.⁹ This study further reported that these NPs display targeted anticancer activity with a minimal toxicity to healthy cells.⁹

It has also been observed that AgNPs can upregulate the expression of pro-apoptotic genes, including Bax, Caspase-3 and Caspase-7, while downregulating anti-apoptotic genes such as Bcl-2 and Bcl-XI which are involved in apoptotic process.^{12,25}

Antioxidant properties

Among the chamomile-synthesized NPs discussed, Ag NPs, Cu NPs and ZnO NPs have been evaluated for their antioxidant activity. Ag NPs achieved nearly 100 % inhibition at the concentration of 1000 μ g/mL with an IC_{50} of 37 μ g/mL.²² In contrast, another study reported that Ag NPs mixed with an equal volume of DPPH (1,1Diphenyl 2-picryl hydrazine) solution showed only 11.23 ± 0.82 % inhibition.¹² Notably, Abdellatif et al. observed that chamomile extract exhibited greater antioxidant activity than the synthesized AgNPs in the DPPH assay, whereas in the FRAP method, AgNPs demonstrated slightly higher reducing activity than the plant extract. Additionally, chamomile-based AgNPs were more effective in reducing molybdate ions compared to chamomile extract, with total antioxidant activity (TAA) values of 36.65 ± 0.88 and 31.33 ± 0.83 , respectively.¹² It has been demonstrated that the antioxidant efficiency of NPs depends on their concentration.³³ For instance, the lowest concentration of ZnONPs synthesized using *M. chamomilla* extract (0.1 mg/mL) scavenged 52.7 % of

ABTS ((2,2'-azino-bis(3-ethylbenzothiazoline-6-sulfonic acid)) free radicals and 54.1 % of DPPH free radicals, while the highest concentration (1.5 mg/mL) showed 78.8 % and 72.7 % scavenging activity against ABTS and DPPH radicals, respectively. Moreover, the chamomile extract alone showed significantly lower antioxidant activity compared to its NPs activity. In addition to chamomile-mediated NPs, Shabir et al. also tested ZnO NPs synthesized with *Urtica dioica* and *Murraya koenigii* extracts, observing that the extracts richer in phenolics and flavonoid exhibited higher antioxidant activity, a trend also reflected in their respective NPs.³³ Similarly, chamomile-based CuO NPs recorded a reducing capacity of 87.27 % at a concentration of 60 ppm.¹⁸

Catalytic properties

Environmental remediation

Rhodamine B (RB) is a synthetic dye widely used in textile, plastic, and cosmetic industries and it is well known for its toxicity to humans.³⁸ The photocatalytic activity of chamomile-based Ag NPs was investigated against RB. Their results revealed that 93.37 % of the dye was degraded within 130 minutes, highlighting the potential of biosynthesized NPs as catalytic agents in environmental remediation.²³ The photocatalytic reduction reaction was intended for the degradation of staining fluorescent dye RB using photo-induced biomolecule-assisted AgNPs as photocatalysts under UV light. The phenomenon of photocatalysis is after the competitive mutual recombination and the separation of electron–hole pairs. However, an increase in the electron–hole pair separation in a photocatalytic reduction reaction leads to an increase in photocatalytic activity throughout the lifetime of charge carriers.

The degradation efficiency of RB was influenced by both temperature and pH. At 30 °C in an acidic medium the degradation reached 93.36 %, while at 60 °C and alkaline conditions the efficiency increased to 98.55 %. Interestingly, Pd/Fe₃O₄ NPs obtained from chamomile extract have demonstrated applicability in Suzuki-Miyaura coupling reactions, which are essential for the formation of biaryl compounds used in pharmaceutical and agrochemical industries. The catalyst exhibited high reusability, maintaining its activity over eight consecutive cycles with minimal leaching of palladium (1.2 %), making it economically and environmentally valuable.¹⁶

Pakseresht et al., synthesized chamomile-based TiO₂NPs which exhibited remarkable electrochemical performance. The TiO₂ cathodes achieved a full discharge capacity of 2000 mAh g⁻¹ and a specific capacity of 500 mAh g⁻¹ over 30 stable cycles. Notably, no formation of Li₂CO₃ or side reaction was observed.²⁰ These results suggest that chamomile-based TiO₂NPs represent a promising alternative for lithium battery cathode.

Other properties

Chamomile-based ZnONPs ameliorated the toxic effects of ROT (rotenone) in *Drosophila melanogaster* by enhancing acetylcholinesterase (AChE) activity, resulting in only 43.75 % inhibition compared to 77.92 % inhibition in the control group. Furthermore, the group treated with ZnO NPs in combination with ROT exhibited higher protein content in third instar larvae of *D. melanogaster* (9.06 ± 0.235 mg/g) than the group treated with ROT alone (6.41 ± 0.258 mg/g). In addition, chamomile-synthesized ZnONPs improved cellular viability, memory, and locomotor activity in the ZnONPS plus ROT-treated group compared to the ROT-only group.³³

Conclusions

Chamomile extract represents a valuable resource for the green synthesis of NPs with remarkable properties, such as antimicrobial, antioxidant, cytotoxic, and catalytic activities, which can be widely used in healthcare, agriculture and environmental remediation.

Current limitations, such as variability in nanoparticle characteristics, the lack of standardized protocols, and limited toxicological data, necessitate that future research directions focus on optimizing synthesis, increasing reproducibility, and conducting thorough safety assessments for clinical and industrial applications.

Table 1. Summary of the synthesis, characterization and applications of metals derived from *Matricaria chamomilla* extracts.

Part used	Solvent	Substrate	NPs	Characterization techniques	Shape, size and ζ	Phytoconstituents	Applications	Ref.
Flowers	Ethanol (70 %)	Na ₂ SiO ₃	SiO ₂ NPs	UV-Vis, FTIR, XRD, TEM	Spherical particles; 17-28 nm (TEM); $\zeta = -31$ mV	-OH bond, -C-CH ₃ - bond, -C-CH ₂ - bond, C-O stretching, Si-O and Si-O-Si bending vibrations	Antifungal activity	15
Flowers	Ultrapure water	FeCl ₃ (1 M)	Magnetite NPs	FTIR, PXRD, SEM, magnetometry	Irregular particles; 6-8 nm (PXRD)	Fe-O stretching vibrations, and O-H, C-H, C=C, C-O, C-O-C stretching, O-H bending vibrations (polyphenols, flavonoids and terpenoids)	Cytotoxic activity	9
Leaves	Distilled water	AgNO ₃ (0.001 M)	Ag NPs	UV-Vis, XRD, FE-SEM, TEM	Spherical particles; 10-70 nm (FE-SEM, TEM)	-	Anticancer activity	22
Flowers	Deionized water	AgNO ₃ (1 mM)	Ag NPs	UV-Vis, Zeta Sizer Nano-series	Spherical particles; ~41 nm	-	Antibacterial activity	21
Aerial parts	Distilled water/ethanol (70:30)	AgNO ₃ (2 mM)	Ag NPs	Zeta Sizer, SEM, UV-Vis, FTIR, DLS, PDIs,	Oval-shaped particles; 115 ± 3.1 nm (SEM); $\zeta = -27.3 \pm 3.92$ mV	O-H stretching of phenols, C-H stretching of glucosides, C=O bond, C-O-C stretching of aromatic ethers and polysaccharides, C-O groups of polyols (flavones, terpenoids and polysaccharides)	Antioxidant and anticancer activity	12

Flowers and leaves	Deionized water	$\text{Zn}(\text{NO}_3)_2 \cdot 6\text{H}_2\text{O}$ (0.3 mM)	ZnO NPs	UV-Vis, XRD, FTIR, Zeta potentiometer, DLS, FE-SEM, EDX	Spherical and hexagonal particles; 10.63-90.37 nm (DLS); 29-50 nm (FE-SEM) $\zeta = -18.5$ mV	O-H group vibrations, C-H alkaline vibrations, N=O vibration, C=C stretching vibration, C-O stretching vibration	Antioxidant and antibacterial activity	33
Leaves	Distilled water	$(\text{CH}_3\text{COOH})_2\text{Mn} \cdot 6\text{H}_2\text{O}$	MnO_2 NPs	FTIR, FE-SEM, EDX	Irregular particles; 18.7-79.3 nm (FE-SEM)	O-H stretching, C=O stretching, O-Mn-O stretching bond	Antimicrobial activity	27
Flowers	Distilled water	ZnO (1 M)	ZnO NPs	TEM, FTIR, UV-Vis, SEM,	8.9-32.6 nm (TEM)	O-H stretching vibration, CH_3 stretching vibrations, Cl/4O stretching vibration from amide group, C-O-H bending vibration, C-N stretching vibration	Antibacterial activity	19
Flowers	Deionized water	$\text{FeSO}_4 \cdot 7\text{H}_2\text{O}$ and $\text{FeCl}_3 \cdot 6\text{H}_2\text{O}$ Na_2PdCl_4	Pd/ Fe_3O_4 NPs	FTIR, TEM, EDX, FE-SEM,	Globular particles; 20-50 nm (TEM)	Fe-O bond, O-H, C-H, C=C, C-O, C-O-C stretching, O-H bending vibrations, polyphenols, flavonoids, terpenoids	Catalytic activity	16
Not mentioned	Distilled water	$\text{HAuCl}_4 \cdot 3\text{H}_2\text{O}$	Au NPs	UV-Vis, TEM,	Spherical particles; 20 nm (TEM)	-	-	39
Leaves	Distilled water	AgNO_3 (2 mM)	Ag NPs	TEM, SEM, EDX, XRD, FTIR	Spherical particles; 5-40 nm (TEM)	O-H group of phenols, terpenoids and flavonoids, C-O-C stretch	Catalytic activity	23

Flowers	Distilled water	AgNO ₃ (1 mM)	Ag NPs	UV-Vis, XRD, SEM	Spherical and irregular particles; 18 ±3 nm (SEM)	-	Antibacterial activity	¹⁴
Flowers	Acetone	TTIP	TiO ₂ NPs	UV-Vis, FE-SEM, XRD	Cauliflower morphology; 10-20 nm (FE-SEM)	-	-	²⁰
Flowers	Distilled water	MgO and MgO ₂ (1 M)	MgO NPs MnO ₂ NPs	UV-Vis, FTIR, TEM, SEM, EDS, XRD	Spherical particles; 36.6-112.0 nm (SEM)	O-H bond, C=C stretching, N-H bond, C-H bond, C-O bond, C=O bond	Antibacterial activity	¹⁷
Flowers	Distilled water	ZnO (1 M)	ZnO NPs	UV-Vis, TEM, SEM, FTIR, XRD	Cubic particles; 51.2 ± 3.2 nm (TEM); 49.8-191.0 nm (SEM)	O-H stretching vibrations, CH ₃ stretching vibrations, C=O stretching vibration, C-O-C stretching vibration, C-N stretching vibration	Antibacterial activity	³⁷
Flowers	Distilled water	AgNO ₃ (5 mM)	Ag NPs	UV-Vis, TEM, XRD, SAED	Spherical particles; ~20 nm (TEM)	-	-	²⁸
Leaves	Distilled water	AgNO ₃ (1 mM)	Ag NPs	TEM, FE-SEM, DLS, FTIR, XRD, EDX.	Spherical particles; 25-36 nm (FE-SEM); ~34 nm (TEM); $\zeta = -34$ mV	O-H stretching (phenols and alcohols), C-H aldehydic stretching, amide I vibrations, carbonyl group of amino acids, C-O-C stretching	Anticancer activity	²⁵
Flowers	Distilled water	AgNO ₃ (5 mM)	Ag NPs	SEM, UV-Vis, DLS,	Spherical particles; 30- 70 nm (SEM)	-	Antimicrobial activity	²⁴

Flowers	Distilled water	$\text{Cu}(\text{NO}_3)_2 \cdot 3\text{H}_2\text{O}$ (1 mM)	CuO NPs	UV-Vis, SEM, EDX, XRD, DLS, FTIR, Zeta potential	Spherical particles; 140 ± 10 nm (SEM); $\zeta = -20$ mV	O-H bad vibration, C=C and C=O stretching of aromatics, C-O band,	Antioxidant and DNA cleavage activity	¹⁸
Whole plant	Deionized water	AgNO_3 (20 mM)	Ag NPs	UV-Vis, electron microscopic	Undefined shape; 60-65 nm	-	Antimicrobial activity	²⁶

I

References

1. Singh, O.; Khanam, Z.; Misra, N.; Srivastava, M. Chamomile (*Matricaria chamomilla* L.): An overview. *Phcog. Rev.* **2011**, *5*(9), 82. <https://doi.org/10.4103/0973-7847.79103>
2. Dhaka, A.; Chand Mali, S.; Sharma, S.; Trivedi, R. A review on biological synthesis of silver nanoparticles and their potential applications. *Res. Chem.* **2023**, *6*, 101108. <https://doi.org/10.1016/j.rechem.2023.101108>
3. Oprică, L.; Molchan, O.; Grigore, M.-N. Salinity and selenium nanoparticles effect on antioxidant system and malondialdehyde content in *Ocimum basilicum* L. seedlings. *J. Exp. Mol. Biol.* **2018**, *4*, 99 – 106.
4. Oprică, L.; Bălășoiu, M. Nanoparticles: an overview about their classifications, synthesis, properties, characterization and applications. *J. Exp. Mol. Biol.* **2019**, *4*, 43 – 60.
5. Oprică, L.; Andries, M.; Sacarescu, L.; Popescu, L.; Pricop, D.; Creangă, D.; Bălășoiu, M. Citrate-silver nanoparticles and their impact on some environmental beneficial fungi. *Saudi J. Biol. Sci.* **2020**, *27*(12), 3365 – 3375. <https://doi.org/10.1016/j.sjbs.2020.09.004>
6. Bhardwaj, B.; Singh, P.; Kumar, A.; Kumar, S.; Budhwar, V. Eco-friendly greener synthesis of nanoparticles. *Adv. Pharm. Bull.* **2020**, *10*(4), 566 – 576. <https://doi.org/10.34172/apb.2020.067>
7. Ying, S.; Guan, Z.; Ofoegbu, P. C.; Clubb, P.; Rico, C.; He, F.; Hong, J. Green synthesis of nanoparticles: current developments and limitations. *Environ. Technol. Innov.* **2022**, *26*, 102336. <https://doi.org/10.1016/j.eti.2022.102336>
8. Moores, A. Green synthesis of nanoparticles: pioneering sustainable technologies. *J. Nanosci. Nanotechnol. Res.* **2023**, *7*(2), 12. DOI: [10.12769/IPNNR.23.7.12](https://doi.org/10.12769/IPNNR.23.7.12)
9. Paut, A.; Guć, L.; Vrankić, M.; Crnčević, D.; Šenjug, P.; Pajić, D.; Odžak, R.; Šprung, M.; Nakić, K.; Marciuš, M.; Prkić, A.; Mitar, I.

Plant-mediated synthesis of magnetite nanoparticles with *Matricaria chamomilla* aqueous extract. *Nanomaterials* **2024**, *14*(8), 729. <https://doi.org/10.3390/nano14080729>

10. Lim, T. K. *Edible medicinal and non-medicinal plants, vol. 7, Flowers*; Springer Netherlands: Dordrecht, 2014. <https://doi.org/10.1007/978-94-007-7395-0>

11. El Mihyaoui, A.; Esteves Da Silva, J. C. G.; Charfi, S.; Candela Castillo, M. E.; Lamarti, A.; Arnao, M. B. Chamomile (*Matricaria chamomilla* L.): a review of ethnomedicinal use, phytochemistry and pharmacological uses. *Life* **2022**, *12*(4), 479. <https://doi.org/10.3390/life12040479>

12. Abdellatif, A. A. H.; Mohammed, H. A.; Abdulla, M. H.; Alsubaiyel, A. M.; Mahmood, A.; Samman, W. A.; Alhaddad, A. A.; Al Rugaie, O.; Alsharidah, M.; Vaali-Mohammed, M. A.; Al Hassan, N.; Taha, H. H. Green synthesized silver nanoparticles using the plant-based reducing agent *Matricaria chamomilla* induce cell death in colorectal cancer cells. *Eur. Rev. Med. Pharmacol. Sci.* **2023**, *27*(20), 10112 – 10125. https://doi.org/10.26355/eurrev_202310_34191

13. Haghi, G.; Hatami, A.; Safaei, A.; Mehran, M. Analysis of phenolic compounds in *Matricaria chamomilla* and its extracts by UPLC-UV, *Res. Pharm. Sci.* **2014**, *9*(1), 31 – 7. PMID: 25598797; PMCID: PMC4292179.

14. Mohamedsalih, P.; Sabir, D. Antimicrobial activity of silver nanoparticles with antibiotics against clinically isolated. *Acinetobacter baumannii*, *Passer J.* **2020**, *2*, 51 – 56. <https://doi.org/10.24271/PSR.11>

15. Baka, Z. A. M.; El-Sharkawy, A. M.; El-Zahed, M. M. Anti-*Aspergillus niger* action of biosynthesized silicon dioxide nanoparticles alone or combined with *Matricaria chamomilla* L. extract. *J. Microb. Biotech. Food Sci.* **2024**, *13*(5), e10816. <https://doi.org/10.55251/jmbfs.10816>

16. Veisi, H.; Zohrabi, A.; Kamangar, S. A.; Karmakar, B.; Saremi, S. G.; Varmira, K.; Hamelian, M. Green synthesis of pd/fe3o4 nanoparticles

using *Chamomile* extract as highly active and recyclable catalyst for Suzuki coupling reaction. *J. Organomet. Chem.* **2021**, *951*, 122005. <https://doi.org/10.1016/j.jorgchem.2021.122005>

17. Ogunyemi, S. O.; Zhang, F.; Abdallah, Y.; Zhang, M.; Wang, Y.; Sun, G.; Qiu, W.; Li, B. Biosynthesis and characterization of magnesium oxide and manganese dioxide nanoparticles using *Matricaria chamomilla* L. extract and its inhibitory effect on *Acidovorax oryzae* strain rs-2. *Artif. Cells Nanomed. Biotechnol.* **2019**, *47*(1), 2230 – 2239. <https://doi.org/10.1080/21691401.2019.1622552>

18. Duman, F.; Ocsoy, I.; Kup, F. O. Chamomile flower extract-directed CuO nanoparticle formation for its antioxidant and DNA cleavage properties. *Mater. Sci. Engin. C* **2016**, *60*, 333 – 338. <https://doi.org/10.1016/j.msec.2015.11.052>

19. Khan, R. A. A.; Tang, Y.; Naz, I.; Alam, S. S.; Wang, W.; Ahmad, M.; Najeeb, S.; Rao, C.; Li, Y.; Xie, B.; Li, Y. Management of *Ralstonia solanacearum* in tomato using ZnO nanoparticles synthesized through *Matricaria chamomilla*. *Plant Dis.* **2021**, *105*(10), 3224 – 3230. <https://doi.org/10.1094/PDIS-08-20-1763-RE>

20. Pakseresht, S.; Cetinkaya, T.; Al-Ogaili, A. W. M.; Halebi, M.; Akbulut, H. Biologically synthesized TiO₂ nanoparticles and their application as lithium-air battery cathodes. *Ceram. Int.* **2021**, *47*(3), 3994 – 4005. <https://doi.org/10.1016/j.ceramint.2020.09.264>

21. Elchaghaby, M. A.; Rashad, S.; Yousry, Y. M. Inhibitory effect of silver nanoparticles synthesized using the chamomile extract against *Streptococcus mutans* cariogenic pathogen. *Dent. Med. Probl.* **2023**, *60* (3), 483 – 488. <https://doi.org/10.17219/dmp/152063>

22. Yu, S.; Zhao, L.; Kang, W.; Amirpour Amraii, S. Characterization and cytotoxicity, antioxidant, and anti-lung carcinoma effects of *Matricaria chamomilla* extract green-synthesized ag nanoparticles: describing a modern chemotherapeutic supplement. *Inorg. Chem. Commun.* **2024**, *168*, 112904. <https://doi.org/10.1016/j.inoche.2024.112904>

23. Alshehri, A. A.; Malik, M. A. Phytomediated photo-induced green synthesis of silver nanoparticles using *Matricaria chamomilla* L. and its catalytic activity against Rhodamine B. *Biomolecules* **2020**, *10*(12), 1604. <https://doi.org/10.3390/biom10121604>

24. Dogru, E.; Demirbas, A.; Altinsoy, B.; Duman, F.; Ocsoy, I. Formation of *Matricaria chamomilla* extract-incorporated Ag nanoparticles and size-dependent enhanced antimicrobial property. *J. Photochem. Photobiol. B Biol.* **2017**, *174*, 78 – 83. <https://doi.org/10.1016/j.jphotobiol.2017.07.024>

25. Dadashpour, M.; Firouzi-Amandi, A.; Pourhassan-Moghaddam, M.; Maleki, M. J.; Soozangar, N.; Jeddi, F.; Nouri, M.; Zarghami, N.; Pilehvar-Soltanahmadi, Y. Biomimetic synthesis of silver nanoparticles using *Matricaria chamomilla* extract and their potential anticancer activity against human lung cancer cells. *Mater. Sci. Eng. C* **2018**, *92*, 902 – 912. <https://doi.org/10.1016/j.msec.2018.07.053>

26. Negahdary, M.; Omidi, S.; Eghbali-Zarch, A.; Mousavi, S. A. Plant synthesis of silver nanoparticles using *Matricaria chamomilla* plant and evaluation of its antibacterial and antifungal effects. *Biomed. Res.* **2015**, *26*(4), 794 – 799.

27. Sabeha, S.; J. Shanan, Z. Synthesis of manganese dioxide nanoparticles by plant extract mediated and their effect on biofilm formation. *IHJPAS* **2023**, *36*(3), 91 – 99. <https://doi.org/10.30526/36.3.3061>

28. Mladenova, B.; Diankov, S.; Karsheva, M.; Stankov, S.; Hinkov, I. Plant mediated synthesis of silver nanoparticles using extracts from *Tilia cordata*, *Matricaria chamomilla*, *Calendula officinalis* and *Lavandula angustifolia* flowers. *J. Chem. Technol. Metall.* **2018**, *53*(4), 623 – 630.

29. Nagalakshmi R. Reddy, K. S. G. A detailed review on green synthesis of silver nanoparticles of chamomile extract with antifungal properties. *Int. J. Pharm. Sci.*, **2024**, *2*(8), 2941 – 2956. <https://doi.org/10.5281/ZENODO.13293136>

30. Titus, D.; James Jebaseelan Samuel, E.; Roopan, S. M. Nanoparticle characterization techniques. In *Green synthesis, characterization and applications of nanoparticles*, Editor(s): Ashutosh Kumar Shukla, Siavash Iravani, Elsevier, 2019; pp 303 – 319.
<https://doi.org/10.1016/B978-0-08-102579-6.00012-5>

31. Umaralikhan, L.; Jamal Mohamed Jaffar, M. Green synthesis of MgO nanoparticles and antibacterial activity. *Iran J. Sci. Technol. Trans. Sci.* **2018**, 42(2), 477 – 485. <https://doi.org/10.1007/s40995-016-0041-8>

32. Wang, H.; Adeleye, A. S.; Huang, Y.; Li, F.; Keller, A. A. Heteroaggregation of nanoparticles with biocolloids and geocolloids. *Adv. Colloid Interface Sci.* **2015**, 226, 24 – 36.
<https://doi.org/10.1016/j.cis.2015.07.002>

33. Shabir, S.; Sehgal, A.; Dutta, J.; Devgon, I.; Singh, S. K.; Alsanie, W. F.; Alamri, A. S.; Alhomrani, M.; Alsharif, A.; Basalamah, M. A. M.; Faidah, H.; Bantun, F.; Saati, A. A.; Vamanu, E.; Singh, M. P. Therapeutic potential of green-engineered ZnO nanoparticles on rotenone-exposed *D. melanogaster* (Oregon R+): unveiling ameliorated biochemical, cellular, and behavioral parameters. *Antioxidants* **2023**, 12(9), 1679. <https://doi.org/10.3390/antiox12091679>

34. Rodríguez, K.; Araujo, M. Temperature and pressure effects on zeta potential values of reservoir minerals. *J. Colloid Interface Sci.* **2006**, 300(2), 788 – 794. <https://doi.org/10.1016/j.jcis.2006.04.030>

35. Serrano-Lotina, A.; Portela, R.; Baeza, P.; Alcolea-Rodriguez, V.; Villarroel, M.; Ávila, P. Zeta potential as a tool for functional materials development. *Catal. Today* **2023**, 423, 113862.
<https://doi.org/10.1016/j.cattod.2022.08.004>

36. Tripathi, P.; Gajbhiye, S.; Agrawal, G. Clinical and antimicrobial profile of *Acinetobacter* spp.: an emerging nosocomial superbug. *Adv. Biomed. Res.* **2014**, 3(1), 13. <https://doi.org/10.4103/2277-9175.124642>

37. Ogunyemi, S. O.; Abdallah, Y.; Zhang, M.; Fouad, H.; Hong, X.; Ibrahim, E.; Masum, Md. M. I.; Hossain, A.; Mo, J.; Li, B. Green

synthesis of zinc oxide nanoparticles using different plant extracts and their antibacterial activity against. *Xanthomonas oryzae* pv. *oryzae*, *Artif. Cells Nanomed. Biotechnol.* **2019**, *47*(1), 341 – 352.
<https://doi.org/10.1080/21691401.2018.1557671>

38. Zhang, D.; Pu, H.; Huang, L.; Sun, D.-W. Advances in flexible surface-enhanced Raman scattering (SERS) substrates for nondestructive food detection: fundamentals and recent applications. *Trends Food Sci. Technol.* **2021**, *109*, 690 – 701.
<https://doi.org/10.1016/j.tifs.2021.01.058>

39. Chávez-Sandoval, B. E.; Flores-Mendoza, N.; Chávez-Recio, A.; Balderas-López, J. A.; García-Franco, F. Biosynthesis of gold nanoparticles (AuNps) and the reducing agents in the process. *Mundo nano* **2021**, *14*(27), 1e – 11e.
<https://doi.org/10.22201/ceich.24485691e.2021.27.69658>